

Statistical Mechanics and Thermodynamics of Simulated Ionic Solutions

M. D'Alessandro,[†] M. D'Abramo,[†] G. Brancato,[†] A. Di Nola,[†] and Andrea Amadei*[‡]

Dipartimento di Chimica, Università di Roma "La Sapienza", P.le Aldo Moro 5, 00185 Roma, Italy, and Dipartimento di Scienze e Tecnologie Chimiche, Università di Roma "Tor Vergata", via della Ricerca Scientifica, 1 I-00133 Roma, Italy

Received: June 13, 2002; In Final Form: August 27, 2002

In this work we combine molecular dynamics simulations with the quasi-Gaussian entropy (QGE) theory to model the statistical mechanics and thermodynamics of ionic solutions. Results showed that the use of the gamma state model provides an excellent theoretical description of the solution behavior over a wide range of temperature. Such an approach makes possible, at relatively low computational costs, the evaluation of partial molar properties such as free energy and entropy which require a heavy computational effort to be estimated with the usual procedures.

Introduction

Accurate methods to obtain the statistical mechanics and thermodynamics of simulated condensed systems are clearly of great importance as they can provide essential information for describing and predicting the behavior of a molecular complex system. Despite the great importance of the development of the simulation methods, the evaluation of essential thermodynamic properties, such as free energy and entropy, and of many related observables, are very difficult, and typically the methodologies used can only provide limited "local" information, i.e., a few thermodynamic properties at a given temperature and density, requiring a rather heavy computational effort. Moreover, the basic theoretical principles underlining these methods, i.e., thermodynamic integration (TI) and cumulant expansion (CE), can be affected by severe problems due to the slow convergence of the average derivatives involved in TI or the physical incoherence of the truncated expansion used in CE. It is therefore a challenge in theoretical physical chemistry to develop and optimize more analytical methods on the bases of sound theories, providing the thermodynamics of a simulated system at relatively low computational costs. In this paper we use the quasi-Gaussian entropy (QGE)¹ theory to describe the complete thermodynamics of a solute–solvent system. Such a theoretical method was recently successfully applied to obtain the statistical mechanics and thermodynamics of flexible molecules simulated in vacuo.² In this work we extend this approach in order to obtain partial molar properties for a liquid mixture defined by a solvent and a highly diluted solute.

Theory

Basic Derivations. For a fluid state system of N solute molecules at high dilution, the partition function can be expressed as^{3,4}

$$Q = \frac{(8\pi^2 V)^N}{N!} (\Theta \int^* e^{-\beta \mathcal{U}'} \prod_{j=1}^n (\det \tilde{m}_j)^{1/2} (\det \tilde{M})^{1/2} d\mathbf{x}_{\text{in}} d\mathbf{x})^N \quad (1)$$

where \mathcal{U}' is the excess energy, basically the potential energy

of the system including the quantum vibrational ground-state energy, V the overall volume of the system, \mathbf{x}_{in} the generalized internal (classical) coordinates of a single solute molecule with fixed rototranslational coordinates, and \mathbf{x} the (classical) coordinates of the n solvent molecules within the solute molecular volume V/N , i.e., the integration limits are defined by V/N . Moreover \tilde{m}_j is the mass tensor of the j th solvent molecule, \tilde{M} the mass tensor of the solute, and Θ a temperature-dependent factor including the quantum corrections, defined as follows:⁴

$$\Theta = \frac{(2\pi kT)^{(d+d_s)/2} (Q_{\text{ref},s}^{\text{qm}})^n Q_{\text{ref}}^{\text{qm}}}{n! h^{(d+d_s)} (1+\gamma)(1+\gamma_s)^n} \quad (2)$$

with $1+\gamma$ and $1+\gamma_s$ the symmetry coefficient for the solute and the solvent respectively, d and d_s the number of classical degrees of freedom in the solute, and n solvent molecules and $Q_{\text{ref},s}^{\text{qm}}$ and $Q_{\text{ref}}^{\text{qm}}$ the solvent and solute molecular quantum vibrational partition functions, respectively, as defined in previous papers.^{1,4} Finally, the star denotes an integration only over the accessible configurational space of the system as obtained within the solute molecular volume V/N . Defining a reference condition as the system at the same temperature and density but without excess energy, with partition function

$$Q_{\text{ref}} = \frac{(8\pi^2 V)^N}{N!} (\Theta \int^* \prod_{j=1}^n (\det \tilde{m}_j)^{1/2} (\det \tilde{M})^{1/2} d\mathbf{x}_{\text{in}} d\mathbf{x})^N \quad (3)$$

we can express the excess (Helmoltz) free energy $A' = A - A_{\text{ref}} = -kT \ln Q/Q_{\text{ref}}$ as¹⁻⁵

$$A' = -NkT \ln \left\{ \frac{\int^* e^{-\beta \mathcal{U}'} \prod_{j=1}^n (\det \tilde{m}_j)^{1/2} (\det \tilde{M})^{1/2} d\mathbf{x}_{\text{in}}}{\int^* \prod_{j=1}^n (\det \tilde{m}_j)^{1/2} (\det \tilde{M})^{1/2} d\mathbf{x}_{\text{in}}} \right\} - kT \ln \epsilon = -NkT \ln \langle e^{-\beta \mathcal{U}'} \rangle_{\text{ref}} - kT \ln \epsilon = NkT \ln \langle e^{\beta \mathcal{U}'} \rangle - kT \ln \epsilon \quad (4)$$

where ϵ is the fraction of available configurational space²

* To whom correspondence should be addressed. Fax: +39-6-72594328. E-mail: andrea.amadei@uniroma2.it.

[†] Dipartimento di Chimica.

[‡] Dipartimento di Scienze e Tecnologie Chimiche.

$$\epsilon = \frac{\int^* (\det \tilde{M})^{1/2} \prod_{j=1}^n (\det \tilde{m}_j)^{1/2} d\mathbf{x}_{in}}{\int (\det \tilde{M})^{1/2} \prod_{j=1}^n (\det \tilde{m}_j)^{1/2} d\mathbf{x}_{in}} \quad (5)$$

The entropic term due to a possible confinement of the system in configurational space, $k \ln \epsilon$, is usually associated with hard-body excluded volume.¹ The ensemble averages in eq 4 can also be expressed as

$$\langle e^{\beta \mathcal{U}'} \rangle_{\text{ref}} = \int \rho_{\text{ref}}(\mathcal{U}') e^{\beta \mathcal{U}'} d\mathcal{U}' \quad (6)$$

$$\langle e^{\beta \mathcal{U}'} \rangle = \int \rho(\mathcal{U}') e^{\beta \mathcal{U}'} d\mathcal{U}' \quad (7)$$

where $\rho_{\text{ref}}(\mathcal{U}')$, $\rho(\mathcal{U}')$ are the probability distribution functions of the excess energy \mathcal{U}' in the reference and actual conditions. Note that the use of ρ_{ref} or ρ is fully equivalent and for a given model distribution they provide identical results. Instead of using a perturbation expansion, in the QGE theory the free energy is obtained by modeling such a distribution and, hence, its moment generating function^{6,7} or Laplace transform, defined in eqs 6 and 7. Using the central limit theorem and a few basic physical and mathematical principles, we can restrict the set of acceptable distribution functions of a macroscopic system to the subgroup of "quasi-Gaussian" distributions, obtained by the convolution of unimodal-like distributions.^{1,2,5,8} Each model distribution function of the excess energy provides the complete temperature dependence, the statistical state of the system. It has been previously shown^{1,2,9-11} that one of the simplest quasi-Gaussian distribution, the gamma distribution, yields a simple and fully physically acceptable statistical state, providing an excellent model of the fluid state thermodynamics over a wide range of temperature and density (i.e., gas to liquid experimental water and methane and simulated Lennard-Jones fluids and large organic molecules). We can rewrite the total excess free energy as

$$A'(T) = N(na'_s + a') \quad (8)$$

where $na'_s + a'$ is the excess free energy of the system defined by the solute molecular volume which contains n solvent molecules and a single solute molecule, a'_s is the partial molecular excess (Helmoltz) free energy of the solvent and clearly a' is the partial molecular excess (Helmoltz) free energy of the solute. It is worth noting that the solvent and solute partial molecular excess free energies are obtained at fixed pressure p for the actual fluid and not in general at fixed pressure for the reference state. This is because the reference state is defined with the same volume and molecules number of the actual condition. This means, defining with $N_s = Nn$ the total number of solvent molecules,

$$a'_s = \left(\frac{\partial A'}{\partial N_s} \right)_{p,T,N} = \left(\frac{\partial A}{\partial N_s} \right)_{p,T,N} - \left(\frac{\partial A_{\text{ref}}}{\partial N_s} \right)_{p,T,N} = \left(\frac{\partial A}{\partial N_s} \right)_{V,T,N} + \left(\frac{\partial A}{\partial V} \right)_{N_s,T,N} v_s - \left(\frac{\partial A_{\text{ref}}}{\partial N_s} \right)_{V,T,N} - \left(\frac{\partial A_{\text{ref}}}{\partial V} \right)_{N_s,T,N} v_s = \mu'_s - p'v_s \quad (9)$$

$$a' = \left(\frac{\partial A'}{\partial N} \right)_{p,T,N_s} = \left(\frac{\partial A}{\partial N} \right)_{p,T,N_s} - \left(\frac{\partial A_{\text{ref}}}{\partial N} \right)_{p,T,N_s} = \left(\frac{\partial A}{\partial N} \right)_{V,T,N_s} + \left(\frac{\partial A}{\partial V} \right)_{N_s,T,N} v - \left(\frac{\partial A_{\text{ref}}}{\partial N} \right)_{V,T,N_s} - \left(\frac{\partial A_{\text{ref}}}{\partial V} \right)_{N_s,T,N} v = \mu' - p'v \quad (10)$$

$$v_s = \left(\frac{\partial V}{\partial N_s} \right)_{p,T,N} \quad (11)$$

$$v = \left(\frac{\partial V}{\partial N} \right)_{p,T,N_s} \quad (12)$$

$$\mu'_s = \mu_s - \mu_{\text{ref},s} \quad (13)$$

$$\mu' = \mu - \mu_{\text{ref}} \quad (14)$$

$$p' = p - p_{\text{ref}} \quad (15)$$

where p_{ref} is the pressure in the reference state, v and v_s the partial molecular volumes of the solute and solvent in the actual fluid (which are in general different from the ones in the reference state) and μ, μ_{ref} the chemical potential in the actual fluid and in the reference condition, respectively. At high dilution the solvent partial molecular properties and all the intensive thermodynamic properties are virtually identical to the pure solvent ones (hence independent of the solute), and so their derivatives in the solvent molecular number, at fixed pressure, must be virtually zero. Assuming that $na'_s + a'$ can be well modeled by a single gamma state¹ we have

$$na'_s + a' = U'_V - T_0 C'_{V0} \Lambda(T) - kT \ln \epsilon \quad (16)$$

$$\Lambda(T) = \frac{1}{\delta_0} + \frac{T}{T_0 \delta_0^2} \ln \{1 - \delta(T)\} \quad (17)$$

$$\delta(T) = \frac{T_0 \delta_0}{T(1 - \delta_0) + T_0 \delta_0} \quad (18)$$

with U'_0 and C'_{V0} the excess internal energy and heat capacity of the system, defined by a single solute molecule and n solvent ones, at the reference temperature T_0 , $k \ln \epsilon$ the entropy term due to configurational confinement, and δ_0 a dimensionless intensive property¹ independent of the temperature, that in our case (high dilution) is determined by the solvent. The gamma state expressions¹ would then provide any thermodynamic property of such a system. Using the fact that $(\partial \Lambda / \partial N_s)_{p,T,N} = 0$ (high solute dilution), we then obtain

$$\left(\frac{\partial \Lambda}{\partial N_s} \right)_{p,T,N} = \left(\frac{\partial \Lambda}{\partial \delta_0} \right)_T \left[\left(\frac{\partial \delta_0}{\partial N_s} \right)_{V,N} + \left(\frac{\partial \delta_0}{\partial V} \right)_{N,N_s} v_s \right] = 0 \quad (19)$$

and hence

$$v_s = - \frac{(\partial \delta_0 / \partial N_s)_{V,N}}{(\partial \delta_0 / \partial V)_{N,N_s}} \quad (20)$$

The last equation clearly shows that both the solute and solvent partial molecular volumes are, along the isochore, temperature independent. This result points out a specific feature of the gamma state model at high solute dilution. It is worth noting that the use of the more complex multigamma state model, introduced in previous papers^{2,12} and based on the partition of phase space into a set of gamma state regions, may provide temperature dependent partial molecular volumes. From the previous equations, subtracting the solvent partial excess free energy from eq 16, we readily obtain

$$a' = \left(\frac{\partial A'}{\partial N} \right)_{V,T,N_s} + \left(\frac{\partial A'}{\partial V} \right)_{N_s,T,N} v = u'_0 - c'_{V0} T_0 \Lambda(T) - kT \ln \bar{\epsilon} \quad (21)$$

where

$$u'_0 = \left(\frac{\partial U'_0}{\partial N} \right)_{V,T,N_s} + \left(\frac{\partial U'_0}{\partial V} \right)_{N_s,T,N} v \quad (22)$$

$$c'_{v0} = \left(\frac{\partial C'_{v0}}{\partial N} \right)_{V,T,N_s} + \left(\frac{\partial C'_{v0}}{\partial V} \right)_{N_s,T,N} v \quad (23)$$

$$\ln \bar{\epsilon} = \left(\frac{\partial \ln \epsilon}{\partial N} \right)_{V,T,N_s} + \left(\frac{\partial \ln \epsilon}{\partial V} \right)_{N_s,T,N} v \quad (24)$$

are temperature independent (as v is temperature independent) and then correspond to the partial molecular excess internal energy and heat capacity, evaluated at the reference temperature T_0 , and $-kT \ln \bar{\epsilon}$ to the partial molecular excess free energy due to the confinement. Using general thermodynamic relations, the gamma state expressions for the various thermodynamic properties and the fact that the partial molecular volumes are temperature independent, we can obtain any possible thermodynamic property at high dilution, e.g., or the partial internal

$$\left(\frac{\partial U'}{\partial N} \right)_{V,N_s,T} = \left(\frac{\partial U'}{\partial N} \right)_{p,N_s,T} - \left(\frac{\partial U'}{\partial V} \right)_{N,N_s,T} v = \left(\frac{\partial \beta u'}{\partial \beta} \right)_{V/N,n} \quad (25)$$

energy u' and heat capacity c'_v

$$u' = \left(\frac{\partial U'}{\partial N} \right)_{p,N_s,T} = \left(\frac{\partial \beta u'}{\partial \beta} \right)_{V/N,n} = u'_0 + (T - T_0) \frac{c'_{v0} T_0}{T(1 - \delta_0) + \delta_0 T_0}$$

$$c'_v = \left(\frac{\partial C'_v}{\partial N} \right)_{p,N_s,T} = \left(\frac{\partial u'}{\partial T} \right)_{V/N,n} = c'_{v0} \left[\frac{T_0}{T(1 - \delta_0) + \delta_0 T_0} \right]^2$$

Combining Simulation Data with Theory. The previous equations describe how we can use the QGE theory in order to treat partial molecular properties. In this subsection we show how it is possible to combine the general derivations of the previous subsection with accurate molecular simulation data. Equation 8 states that we can obtain the whole thermodynamics of a solute–solvent system, at high solute dilution, only using information from simulations of a single solute molecule embedded in the solvent. Using canonical ensemble simulations in a wide temperature range, we can obtain the excess Helmholtz free energy for a pure solvent system as well as for the same system added of a single solute molecule, i.e., at fixed volume. Assuming a gamma state behavior for both systems we can parametrize the corresponding gamma state models fitting the average excess (potential) energies in temperature,¹ and hence obtain the solute excess chemical potential, excluding the confinement contribution

$$\mu^* = \mu' + kT \ln \bar{\epsilon} = \left(\frac{\partial A^*}{\partial N} \right)_{V,T,N_s} = \Delta A^* \quad (26)$$

$$A^* = A' + kT \ln \epsilon \quad (27)$$

where ΔA^* is the difference between the excess Helmholtz free energies without the confinement terms (confined ideal reduced Helmholtz free energy¹) of the solute–solvent system and the pure solvent one, at fixed volume. Note that the confinement term $k \ln \bar{\epsilon}$, corresponding to a pure entropic term, is due to the presence of unaccessible phase space regions due to hard body contacts. In principle such unaccessible configurations should be characterized by an infinite energy or at least should be separated by the others by an infinite energy barrier. In practice

a confinement behavior is typically present also in systems where no unaccessible regions are strictly present.^{2,11} In this case $k \ln \bar{\epsilon}$ must be regarded as an effective confinement term due to the presence of high energy phase space regions which are virtually unaccessible in the whole temperature range of interest. From eqs 10 and 21 we also have

$$\mu^* = u'_0 - c'_{v0} T_0 \Lambda(T) + p^* v \quad (28)$$

$$p^* = p' - \xi T \quad (29)$$

$$\xi = k \left(\frac{\partial \ln \epsilon}{\partial V} \right)_{N,N_s} \quad (30)$$

where $\Lambda(T)$, p^* , p' , and ξ , being intensive properties, are given by the gamma state obtained by the pure solvent simulations. Fitting μ^* as obtained by eq 26, with eq 28, we can evaluate u'_0 , c'_{v0} , and the partial molecular volume v . In this article we focus on water-ions systems where the confinement behavior can be well described by a hard sphere model.¹ This means that in the infinite temperature limit the excess thermodynamics of the theoretical model we use, will reduce to that of a hard sphere mixture of the same molar fraction. Hence, using the well-known thermodynamic relation

$$v = - \frac{(\partial p / \partial N)_{V,N_s,T}}{(\partial p / \partial V)_{N,N_s,T}} \quad (31)$$

in the infinite temperature limit, where the pressure is given by the equation of state of the hard sphere mixture,¹³ we can obtain the hard sphere radius of the solute. Note that the confinement properties of the solvent, including the solvent hard sphere radius, were obtained using the homogeneous hard sphere equation of state proposed by Carnahan–Starling.^{1,14} From the estimate of the solute hard sphere radius it is straightforward to obtain $(\partial \ln \epsilon / \partial N)_{V,T,N_s}$ via the excess chemical potential of the solute hard sphere in the hard sphere mixture following Lebowitz.¹³ Hence, from eq 24 we can evaluate the free energy confinement term $\ln \bar{\epsilon} = (\partial \ln \epsilon / \partial N)_{p,T,N_s}$ via

$$-kT \left(\frac{\partial \ln \epsilon}{\partial N} \right)_{p,T,N_s} = -kT \left(\frac{\partial \ln \epsilon}{\partial N} \right)_{V,T,N_s} + \xi T v \quad (32)$$

With these results we can reconstruct the whole excess thermodynamics of the system along the isochore.

Simulation Methods

We used four different sets of molecular dynamics (MD) simulations over a wide temperature range (280–1200 K). In the first set we simulated a cubic box of 256 simple point charge (SPC)¹⁵ water molecules, at 55.32 mol/L. In the second and third sets we simulated the same SPC box, adding a single sodium or chloride ion. Finally, in the fourth set we simulated a larger SPC box (2180 molecules) at the same density (55.32 mol/L). All the simulations were performed using Gromacs software package^{16–18} modified to use the isokinetic temperature coupling.¹⁹ This was done in order to obtain results fully consistent with statistical mechanics.^{3,20} For all the simulations the number of steps was 2500000 with three different time step: 2 fs for simulations in the range 280–450 K, 1 fs up to 800 K and 0.5 fs up to 1200 K. Hence the corresponding simulation time lengths are about 5, 2.5 and 1.25 ns. In each simulation the initial 100000 steps were used as equilibration run. The long-range electrostatics was calculated using the particle mesh Ewald (PME) method, with 34 wave vectors in

TABLE 1: Properties of the Theoretical Models, Equation 21, for SPC in the Large Simulation Box (SPC_l), SPC in the Small Simulation Box (SPC), Chloride (Cl), and Sodium (Na)^a

	SPC _l	SPC	Cl	Na
d (nm)	0.2426	0.2426	0.4252	0.3440
v (l/mol)	0.0181	0.0181	0.0456	0.0310
u'_0 (kJ/mol)	-41.354	-41.375	-382.873	-406.368
c'_{v0} (J/mol K)	46.058	46.272	41.021	46.102
δ_0	0.6387	0.6565	0.6565	0.6565

^a Diameter of the molecule d , partial molar volume v , partial molar excess internal energy at the reference temperature u'_0 , and partial molar excess heat capacity at the reference temperature c'_{v0} . Note that the intensive gamma state property δ_0 is always given by the pure solvent model (highly diluted solution).

each dimension and a fourth order cubic interpolation. Note that in the PME procedure the interaction between the ion and its replica is removed; hence, the simulation box, with 256 solvent molecules and a single ion, can be considered at high dilution.

Results

We parametrized our theoretical models, described in the theory section, using only the average potential energy (excess internal energy) and pure solvent pressure in the whole temperature range, i.e., by fitting these values with the corresponding to theoretical models. To reduce the noise due to energy fluctuations and properly compare our results with literature computational data where typically a small simulation box is used, we utilized a small (i.e., 256 molecules) simulation box at the typical liquid water density (55.32 mol/L) over a large temperature range (280–1200 K). To be sure that such a reduced box was not seriously changing the thermodynamics of the system, we compared the results obtained for pure SPC using this small box and a larger one (i.e., 2180 molecules), at the same density and over the same temperature range. In Table 1 we summarize the physical properties defining the gamma state models for SPC and the two ions, see theory section. From the first two columns of the table, where we compare the large and small SPC simulation models, it is evident that these are very similar providing virtually identical thermodynamics. It is also worth noting that the hard sphere diameter we obtained for SPC is a bit smaller than that obtained for experimental water.¹ This is probably due to the fact that SPC molecules have the pair minimum energy at a shorter distance than real water, hence providing a smaller hard core. In Figure 1 we compare the excess internal energy as given by the gamma state model with the simulation results for the pure SPC system. Note that on this scale the energy error bars are too small to be shown. In the same figure we also show the gamma state prediction of the excess Helmholtz free energy. In Figures 2 and 3 we compare, for the same pure SPC system, the gamma state prediction of the specific heat capacity and pressure with the corresponding simulation results computed from the fluctuations of the potential energy (heat capacity) and from the virial (pressure). The error bars reported for the simulation heat capacity, as well as in the other figures, are given by plus and minus one sigma; for pressure the error bars are again too small to be shown. In Figure 2 we also show the gamma state prediction of the excess entropy. From these three figures it is evident the excellent agreement between the theoretical model and simulation data. Interestingly the SPC excess chemical potential at 300 K obtained by our theoretical model is -25.81 kJ/mol which is rather close to its estimate by TI²¹ (about -24 kJ/mol). However, the TI value is higher probably because of the use of cut off

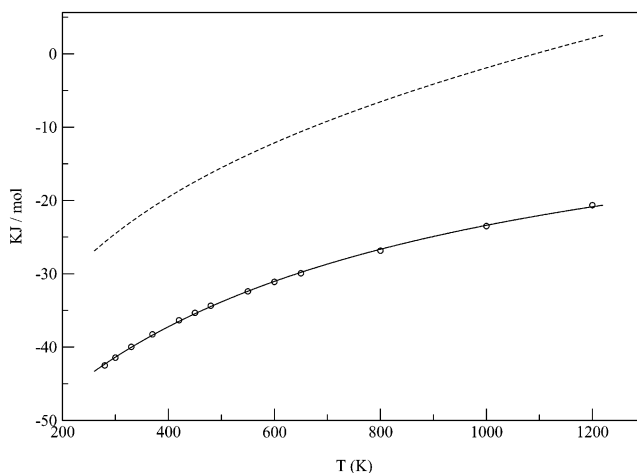


Figure 1. Gamma state prediction of the molecular average potential energy (solid line) and simulation results (circles) for the small box of pure SPC water. In the figure we also show the gamma state prediction of the molecular excess Helmholtz free energy (dashed line), for the same system.

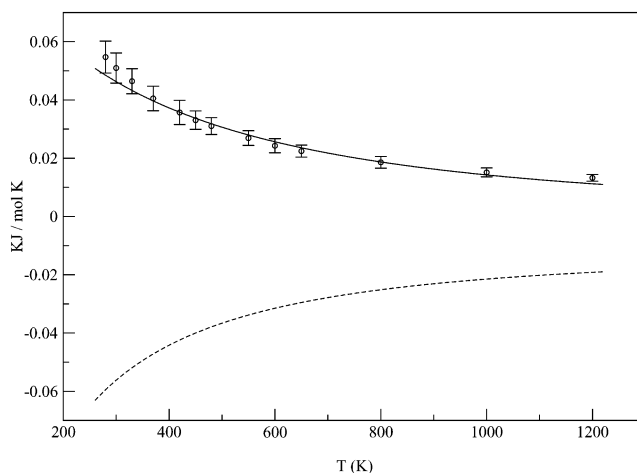


Figure 2. Gamma state prediction of the molecular excess heat capacity (solid line) and simulation results (circles) for the small box of pure SPC water. In the figure we also show the gamma state prediction of the molecular excess entropy (dashed line), for the same system.

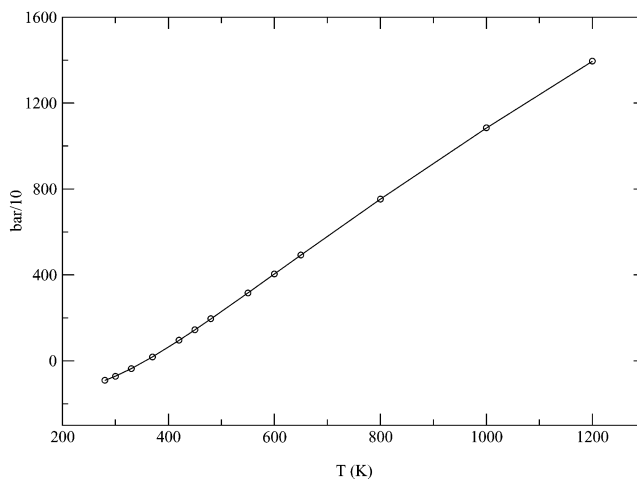


Figure 3. Gamma state prediction of the excess pressure (solid line) and simulation results (circles) for the small box of pure SPC water.

(0.6–1.0 nm) in the simulations. It is worth to note that in the case of the heat capacity at the lowest temperatures there is a possible small (always within one or two sigmas) systematic deviation between the theoretical model and simulation data.

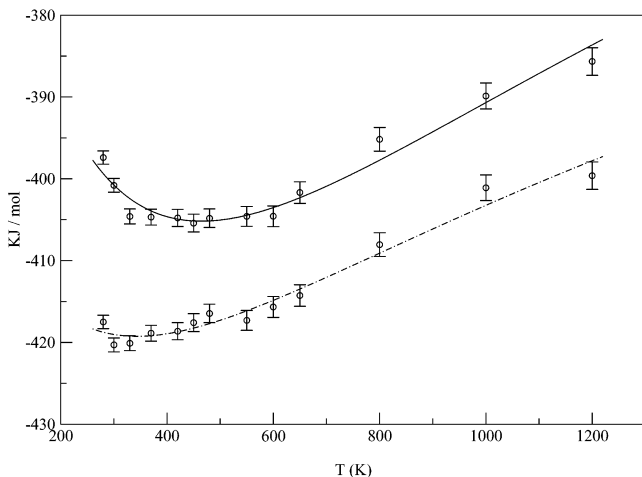


Figure 4. Gamma state predictions and simulation results (circles) of $(\partial U'/\partial N)_{V,T,N_s}$ for chloride ion (solid line) and sodium ion (dot-dashed line).

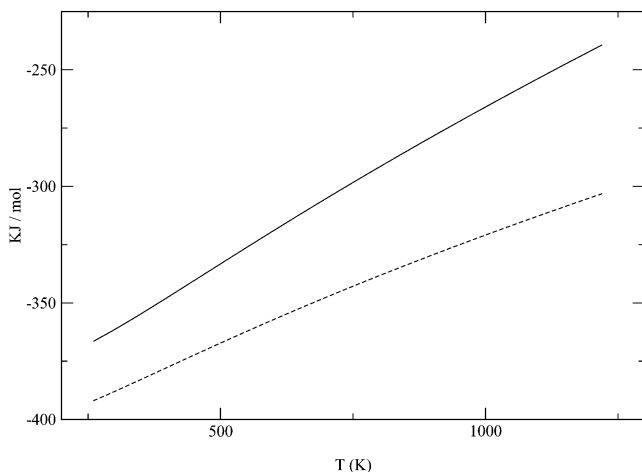


Figure 5. Gamma state predictions of the excess chemical potentials for chloride (solid line) and sodium (dashed line).

This is probably due to the fact that in such a large temperature range phase space regions become accessible which cannot be always described very accurately with a unique gamma state model. Within the temperature range we used in this paper these possible deviations are still within the statistical noise but probably a larger temperature range, resulting in a smaller effective confinement, would require a multigamma state approach.^{2,8,11} In Figure 4 we show the derivative of the average potential energy in the solute molecular number at constant volume for the two ions. Note that this thermodynamic property coincides with the difference of the average potential energies of the systems with and without the ion (we simulated with only one ion as solute). Again the theoretical predictions of the gamma state models, for both solutions, are within the error bars excellent. In the case of chloride we can observe that a well defined minimum is at relatively high temperature suggesting a relevant temperature dependence of the solvent structure close to the ion. This is not the case for sodium where a shallow minimum is present at the lowest temperatures. In Figure 5 the two ions excess chemical potentials, as obtained by the theoretical models, are shown as a function of temperature along the isochore, and in Table 2 we compare these at 298 K with experimental data²² and literature computational results obtained via different types of TI based calculations^{23–25} and via a computational procedure based on a peculiar approximation of the moment generating function (renormalization) providing

TABLE 2: Excess Chemical Potentials for Sodium μ'_{Na^+} and Chloride μ'_{Cl^-} at 298 K as Obtained by Theoretical and Experimental Works

	<i>a</i>	<i>b</i>	<i>c</i>	<i>d</i>	<i>e</i>	<i>f</i>
μ'_{Na^+} (kJ/mol)	−388	−398	−508	−459	−478	−365
μ'_{Cl^-} (kJ/mol)	−362	−371	−315	−237	−365	−340

^a Theoretical results from our work. ^b Theoretical results from Hummer.²³ ^c Theoretical results from Straatsma and Berendsen.²⁴ ^d Theoretical results from Migliore.²⁵ ^e Theoretical results from Jayaram.²⁶ ^f Experimental data from Marcus.²²

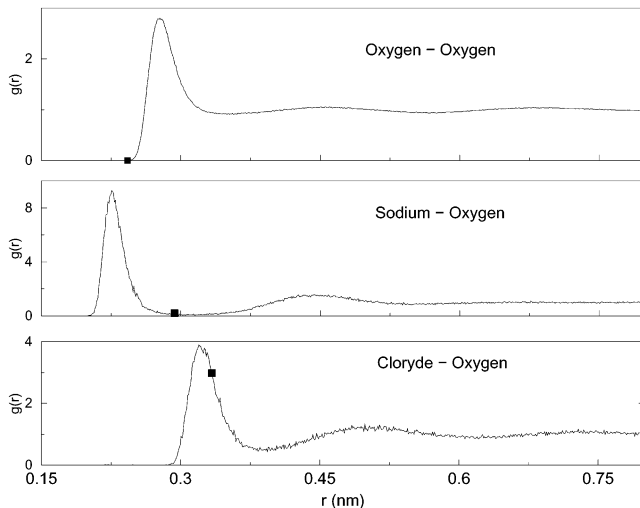


Figure 6. Radial distribution function for the small box of pure SPC water and for the chloride and sodium solute–solvent systems, respectively.

a remarkably simple expression.²⁶ The TI methods require a rather heavy computational effort and thus typically provide only the chemical potential at a single temperature. Interestingly our estimates of the excess chemical potentials at 298 K are very close to recent and sophisticated computational results,²³ and are in reasonable agreement with experimental data.²² Note that no information on the error bars were available in the computational paper²³ and for our model the chemical potential error bars (one sigma) are about 10–15 kJ/mol in the whole temperature range. Finally in Figure 6 we show the radial distribution functions obtained for the pure solvent and the two solute–solvent systems at 300 K. The squares indicate the distance obtained summing the solvent and solute hard core radii as given in Table 1 (in the case of the pure SPC system we consider the SPC hard core diameter). The first curve shows the radial distribution of the pure solvent system and as expected, virtually no SPC molecules can be closer than the hard sphere diameter. In the case of the chloride ion the square is located very close to the maximum of the distribution implying that about half of the first hydration shell is actually involved in the partial molecular volume of this ion. Moreover, the fluctuations of the solvent molecular number within such a distance is not negligible, indicating that the corresponding solvent molecules involved are not rigidly structured around the ion and hence the interaction energy between the ion and solvent is not well optimized. This could perhaps explain the well defined minimum at relatively high temperature of $(\partial U'/\partial N)_{V,T,N_s}$ showed in Figure 4. In the case of sodium the square coincides with the first minimum, meaning that the complete first hydration shell is involved in the partial molecular volume of the ion. In this case the fluctuations of the solvent molecular number within such a distance are quite negligible indicating that the whole first hydration shell is rigidly structured around this ion, as also

shown by the fact that the minimum of the radial distribution is close to zero like for an interface. Interestingly, the estimates of the ionic diameter based on the experimental chemical potential in water, coupled with a simple Born approximation,²⁷ provide for both ions remarkably close values (sodium $d = 0.336$ nm; chloride $d = 0.388$ nm) to our results. On the contrary, these estimates when based on experimental mobility data,²⁸ also in water, provide a good agreement only for sodium but not for chloride which appears to be much smaller (sodium $d = 0.328$ nm; chloride $d = 0.215$ nm). This relevant difference between the “thermodynamic” and “kinetic” radius in the case of chloride could indeed reflect the low rigidity of the solvent molecules close to the ion, as pointed out by the simulation data.

Conclusions

In this paper we showed that the combined use of the QGE theory with MD simulations can provide the whole thermodynamics of a solute–solvent system, including all the partial molar properties. We investigated two ionic solutions, at high dilution, along the typical liquid water isochore. Results showed that within a wide range of temperature the QGE theoretical models provide a coherent and accurate description of all the partial molar properties of solute and solvent as a function of the temperature. Comparison with recent TI based calculations²³ at 298 K shows a remarkable agreement, although the two methods are completely different. Interestingly, from the partial molar volumes, obtained by the theoretical models, and the simulation radial distributions it was also possible to characterize the first hydration shell around the ions, finding a very different behavior between chloride and sodium, in agreement with experimental data. We expect this theoretical approach, in combination with MD simulations, to be efficient in the evaluation of the statistical mechanics and thermodynamics of complex systems where TI based methods, which are presently used, typically provide a limited number of thermodynamic properties at single state points. Difficulties could arise from the complexity of the energy fluctuations in flexible solutes and from the non hard sphere confinement behavior due to complex shapes and charge distributions. However, such possible problems could be solved by the use of the multigamma state model to correctly describe the energy fluctuations, and by more sophisticated hard body equations of state or even direct computational evaluation to obtain a good estimate of the confinement term.

Acknowledgment. We acknowledge Dr. M. E. F. Apol for the useful and stimulating discussions. This work was supported by the European Community Research Training Network Program “Protein (mis)-folding” and PRIN 2001 “Structural Biology and Dynamics of Redox Proteins”.

References and Notes

- (1) Amadei, A.; Apol, M. E. F.; Berendsen, H. J. C. *J. Chem. Phys.* **1997**, *106*, 1893–1912.
- (2) Amadei, A.; Iacono, B.; Grego, S.; Chillemi, G.; Apol, M. E. F.; Paci, E.; Delfini, M.; Di Nola, A. *J. Phys. Chem. B* **2001**, *105*.
- (3) Amadei, A.; Chillemi, G.; Ceruso, M. A.; Grottesi, A.; Di Nola, A. *J. Chem. Phys.* **2000**, *112*, 9–23.
- (4) Amadei, A.; Apol, M. E. F.; Brancato, G.; Di Nola, A. *J. Chem. Phys.* **2002**, *116*, 4437–4449.
- (5) Apol, M. E. F.; Amadei, A.; Berendsen, H. J. C.; Di Nola, A. *J. Chem. Phys.* **1999**, *111*, 4431–4441.
- (6) Patel, J. K.; Kapadia, C. H.; Owen, D. B. *Handbook of Statistical Distributions*; Marcel Dekker: New York, 1976.
- (7) Stuart, A.; Ord, J. K. *Kendall's Advanced Theory of Statistics*, 5th ed.; Griffin: London 1987; Vol. 1.
- (8) Apol, M.; Amadei, A. In preparation.
- (9) Apol, M. E. F.; Amadei, A.; Berendsen, H. J. C. *Chem. Phys. Lett.* **1996**, *256*, 172–178.
- (10) Roccatano, D.; Amadei, A.; Apol, M. E. F.; Di Nola, A.; Berendsen, H. J. C. *J. Chem. Phys.* **1998**, *109*, 6358–6363.
- (11) Amadei, A.; Apol, M. E. F.; Chillemi, G.; Berendsen, H. J. C.; Di Nola, A. *Mol. Phys.* **1999**, *96*, 1469–1490.
- (12) Apol, M. E. F.; Amadei, A.; Berendsen, H. J. C. *J. Chem. Phys.* **1996**, *104*, 6665–6678.
- (13) Lebowitz, J. L.; Rowlinson, J. S. *J. Chem. Phys.* **1964**, *41*, 133–138.
- (14) Carnahan, N. F.; Starling, K. E. *J. Chem. Phys.* **1969**, *51*, 635–636.
- (15) H. J. C. Berendsen, J. P. M. Postma, W. F. v. G.; Hermans, J. *Intermolecular Forces*; Pullmann, B., Ed.; D. Reider Publishing Company: Dordrecht, 1981; pp 331–342.
- (16) van der Spoel, D.; van Drunen, R.; Berendsen, H. J. C. *Groningen MACHINE for Chemical Simulations*; Department of Biophysical Chemistry, BIOSON Research Institute: Nijenborgh 4 NL-9717 AG, Groningen, The Netherlands, 1994. E-mail: gromacs@chem.rug.nl.
- (17) van der Spoel, D.; van Buuren, A. R.; Apol, E.; Meulenhoff, P. J.; Tieleman, D. P.; Sijbers, A. L. T. M.; van Drunen, R.; Berendsen, H. J. C. *Gromacs User Manual Version 1.3*; Department of Biophysical Chemistry, BIOSON Research Institute: Nijenborgh 4 NL-9717 AG, Groningen, The Netherlands, 1996. Internet: <http://rugmd0.chem.rug.nl/gm> × 1996.
- (18) van Gunsteren, W. F.; Billeter, S. R.; Eising, A. A.; Hünenberger, P. H.; Krüger, P.; Mark, A. E.; Scott, W. R. P.; Tironi, I. G. *Biomolecular Simulation: The GROMOS96 Manual and User Guide*; Hochschulverlag AG an der ETH Zürich: Zürich, 1996.
- (19) Evans, D. J.; Morriss, G. P. *Statistical Mechanics of Nonequilibrium Liquids*; Academic Press: London, 1990.
- (20) D'Alessandro, M.; Tenenbaum, A.; Amadei, A. *J. Phys. Chem. B* **2002**, *106*, 5050–5057.
- (21) Hermans, J.; Pathiaseril, A.; Anderson, A. *J. Am. Chem. Soc.* **1988**, *110*, 5982–5986.
- (22) Marcus, Y. *J. Chem. Soc., Faraday Trans.* **1991**, *87*, 2995.
- (23) Hummer, G.; Pratt, L. R.; Garcia, A. E. *J. Phys. Chem. B* **1996**, *100*, 1206–1215.
- (24) Straatsma, T. P.; Berendsen, H. J. C. *J. Chem. Phys.* **1988**, *89* (9), 5876–86.
- (25) Migliore, M.; Corongiu, G.; Clementi, E.; Lie, G. C. *J. Chem. Phys.* **1988**, *88*, 7766.
- (26) Jayaram, B.; Beveridge, D. L. *J. Phys. Chem.* **1990**, *94*, 7288–7293.
- (27) Daune, M. *Molecular Biophysics*; Oxford University Press: Oxford, 1999.
- (28) Atkins, P. *Physical Chemistry*; Oxford University Press: Oxford, 1998.